Spectroscopic Studies on the Competitive Interaction between Polystyrene Sodium Sulfonate with Polycations and the *N*-Tetradecyl Trimethyl Ammonium Bromide Surfactant

I. Estrela-Lopis,*,† J. J. Iturri Ramos,‡ E. Donath,† and S. E. Moya*,‡

Institute of Medical Physics and Biophysics, University of Leipzig, Leipzig, Germany, and CIC biomaGUNE, Paseo Miramón 182 Edificio Empresarial C, 20009 San Sebastian, Gipuzkoa, Spain

Received: September 6, 2009; Revised Manuscript Received: November 6, 2009

The interaction of *N*-tetradecyl trimethyl ammonium bromide (TTAB) surfactants with poly(sodium styrene sulfonate) (PSS), PSS/poly(allylamine hydrochloride) (PAH), and PSS/poly(diallyl dimethyl ammonium chloride) (PDADMAC) complexes has been studied by means of Raman and IR spectroscopy. The stoichiometry of the polyelectrolyte complexes and of the complexes with TTAB has been established. TTAB molecules bind to single PSS molecules in a coiled liquid-like alkyl configuration up to a molar fraction of 67% in dry state. At higher concentrations, TTAB shows a transition to a crystalline phase. In the case of PSS being complexed with PAH, surfactant binds to PSS with a stoichiometry of 2 molecules of TTAB per sulfonic acid group. Spectroscopic data show that TTAB interacting with PSS/PDADMAC complexes is capable of disassembling this polyelectrolyte complex, but when TTAB interacts with the PSS/PAH complexes this polyelectrolyte pair remains stable. Spectroscopic measurements performed at different humidity showed that dry PSS/PAH complexes display the $\nu(SO_2)$ and $\nu_s(SO_3^-)$ bands at positions, which are indicative of the presence of hydrogen bonds between PSS and PAH. Red shifts of these bands when mixing the PSS/PAH complexes with TTAB point to structural rearrangements of the complex when interacting with the surfactant.

Introduction

Polyelectrolyte (PE) complexes and surfactants have many practical and industrial applications in detergency or as part of formulations in cosmetics, paints, and even food products.[1−3] Also, the interaction of surfactants with biological polyelectrolytes like DNA or proteins is a very important tool in the preparation, analysis, and encapsulation of biopolymers.[4−6]

From a physicochemical point of view, the interaction of polyelectrolytes with surfactants raises issues related to colloidal stability, conformational freedom of macromolecules, ordering in self-assembled systems, etc.[7−10] Besides, polyelectrolyte−surfactant complexes (PSC) themselves represent interesting self-assembled structures ranging from bead-like structures to polymer decorated elongated micelles/rods, nanoparticles, or surfactant bilayers,[11−16] controlled by electrostatic, hydrophobic, and entropic forces. The surfactants may determine the degree of order and the spatial arrangement of the polyelectrolyte (PE) molecules.[17−19] Polyelectrolyte−surfactant assemblies are applied in nanotechnology for the functionalization of surfaces,[20,21] for tuning surface wettabilities,[22] and for incorporation of antimicrobial agents.[23] PSC can be used as carriers for non-charged species, such as organic dyes and nanoparticles.[24]

In most studies, PSC have been formed in solution from free polyelectrolyte molecules. The interaction of surfactants with polyelectrolyte multilayer films has been investigated more seldom.[22,24,25] Recently, we have shown that the quaternary surfactant *N*-tetradecyl trimethyl ammonium bromide (TTAB) can be used to selectively strip off poly(diallyl dimethyl ammonium chloride) (PDADMAC)/poly(styrene sodium sulfonate) (PSS) polyelectrolyte multilayers fabricated by means of the layer-by-layer technique of polyelectrolyte assembly.[26] It was demonstrated that, although binding of TTAB to PSS in the multilayer takes place, poly(allyl amine hydrochloride) (PAH)/PSS films remain stable in the presence of TTAB. The different response of PDADMAC/PSS and PAH/PSS multilayer films with regard to their stability to TTAB may thus be related to the strength of the amine sulfonate interaction. The charge of PDADMAC is brought about by quaternary amines being part of a planar ring, which restricts the conformational freedom of the polymer. PAH on the other hand carries primary amines, which are protonated at acid and neutral pH. Additionally, the PAH chain may undergo almost free rotation around the C−C bonds, proving great conformational flexibility to the polymer. The competition between the cationic surfactant on one hand and the polycation interacting with the polyanion on the other hand is an interesting issue. It may depend on a variety of parameters. How the interaction between the two oppositely charged polyions is affected by the interfering surfactant is to our knowledge a largely unexplored subject.

In the present study, we have investigated both in solution and in the dry state polyelectrolyte complexes produced by mixing polycations with polyanions. Bearing in mind the similarity of the PE multilayers with PE complexes, we have used complexes of PDADMAC/PSS and PAH/PSS to study the interaction between PSS and TTAB, in the presence of the two mentioned polycations, by means of Raman microscopy and attenuated total reflection Fourier-transform infrared spectroscopy (ATR-FTIR). Recently, FTIR has been successfully used to study the role of H-bridges and binding mechanisms in phospholipid/PE complexes.[27] The spectroscopic studies presented in the current article allow us to get insight into the molecular mechanism, binding sites, and stoichiometry of the interaction in PSC. The role of the water and hydrogen bonds between the polycations and polyanions for the stability of polyelectrolyte complexes is analyzed. The presence of surfactant results in conformational changes of the PE complexes.

* Corresponding author. E-mail: smoya@cicbiomagune.es.
† University of Leipzig.
‡ CIC biomaGUNE.

10.1021/jp908608u
Published on Web 11/25/2009

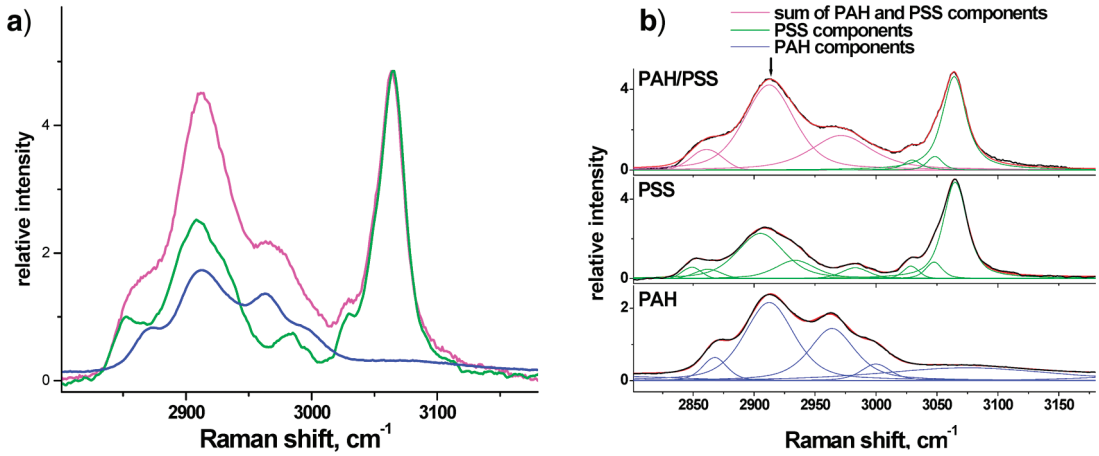

Figure 1. (a) Raman spectra of PAH/PSS (red), PSS (green), and their difference (blue) almost coinciding with the PAH spectrum. (b) Decomposition of the Raman spectra of PAH/PSS complexes and of PSS and PAH into components. The black line refers to the respective recorded spectra; the red lines denote the fits, respectively.

This increased the number of H-bonds between PAH and PSS, while for the PDADMAC/PSS complex, decomposition was observed.

Experimental Section

Materials. Poly(sodium 4-styrene sulfonate) [$M_w \approx 70\,000$], poly(allylamine hydrochloride) [$M_w \approx 15\,000$], and poly(diallyl dimethyl ammonium chloride) 20% in water [$M_w = 2 \times 10^5$ to 3.5×10^5] were purchased from Aldrich. *N*-Tetradecyl (myristyl) trimethyl ammonium bromide (TTAB), ≥98%, quaternary salt, was purchased from Fluka.

Methods. ***Preparation of PE Complexes and PSC.*** Complexes of PAH/PSS and PDADMAC/PSS were prepared at different molar ratios in 0.5 M NaCl, centrifuged three times, followed by removal of the supernatant. Varying amounts of TTAB were added to the PE complexes. Afterward, these PSC were centrifuged and washed three times. The initial TTAB concentration was 100 mM, which is considerably above the critical micelle concentration (CMC). The TTAB micelles at this concentration in aqueous solutions have a shape of prolate ellipsoids with half axes of 18 and 35 Å, respectively.[28]

Raman Microscopy. Micro-Raman analyses were performed using a Renishaw inVia Raman microscope. The laser excitation wavelength was 532 nm with a grating of 1800 mm^{-1}. The microscope was equipped with interchangeable objective lenses with magnifications of 10×, 50×, and 100×. Most measurements were conducted using the 50× objective. The size of the focal spot was approximately 1 μm. Raman spectra were recorded in the region 300−3600 cm^{-1} with a spectral resolution of around 7 cm^{-1}. These measurements cover both the fingerprint and the CH stretch vibration region. Two to eight accumulation scans at different sample points were used to reduce the spectral noise and to account for possible sample inhomogeneities. The system was calibrated to the spectral line of crystalline silicon at 520.7 cm^{-1}. All spectra were baseline corrected. The PE complexes and PSC, observed by reflectance microscopy, were dispersed on silica slides to minimize the fluorescence background. Raman spectra were measured directly under the microscope in solution and dry state at room temperature. The confocal modus was applied in the case of strong fluorescence.

ATR-FTIR. Polyelectrolytes were deposited onto the surface of a ZnSe ATR crystal mounted into a commercial horizontal ATR holder. The degree of hydration of the PE film was adjusted by means a moisture generator (HumiVar, Leipzig, Germany) to relative humidity (RH) values between 3% and 99% with an accuracy of ±0.5%. IR spectra were recorded by means of the Excalibur FTS3100 Fourier transform IR spectrometer (Varian, Darmstadt, Germany) with a resolution of 4 cm^{-1} from 100 scans at room temperature.

Results and Discussion

1. Stoichiometric Composition of PE Complexes. It can be expected that the quaternary ammonium surfactant TTAB will compete with polycations for the PSS binding sites. The number of free sulfonate groups and groups taking part in the interaction with the polycations depends in a straightforward way on the initial stoichiometric ratio of the complex forming constituents. Stable complexes can exist only if one of the constituents has been added with a concentration in excess; otherwise, flocculation cannot be controlled. Because the competitive interaction with TTAB was in the focus of our interest, PSS was added in excess to obtain stable negatively charged polyelectrolyte complexes. In all subsequent experiments, the polyelectrolyte complexes were formed by mixing PSS with PAH in a ratio of either 3:1 or 5:1 (monomer/monomer), respectively. Because the stoichiometry of the formed complexes may not be identical to the applied monomer ratios, we first determined the stoichiometry of the complexes from analyzing the respective Raman spectra. The soluble excess of PSS, which has not been utilized for complex formation, was largely removed by the applied centrifugation/washing cycles while the complexes were retained and subsequently dried. The respective vibration spectra of PSS, PAH, PDADMAC, and the complexes of PAH/PSS and PDADMAC/PSS were recorded afterward.

The spectra of PSS and PAH/PSS weighted on the integral intensity of the PSS aromatic band are shown in Figure 1a. The spectrum of the complex can thus be considered to be largely a superposition of its constituents.

The spectra of the individual dry polyelectrolytes can be used to deconvolute the spectrum of the PAH/PSS complex. The contribution of the respective PAH and PSS components to the aliphatic band integral intensity with its center at $\nu_{as}^{CH2} = 2905$ cm^{-1} denoted by an arrow in Figure 1b was calculated from the spectrum decomposition. The Voigt function was used for fitting the spectra. It was found that the intensity ratio of the PAH and PSS CH_2 vibration bands is very close to 1:1.

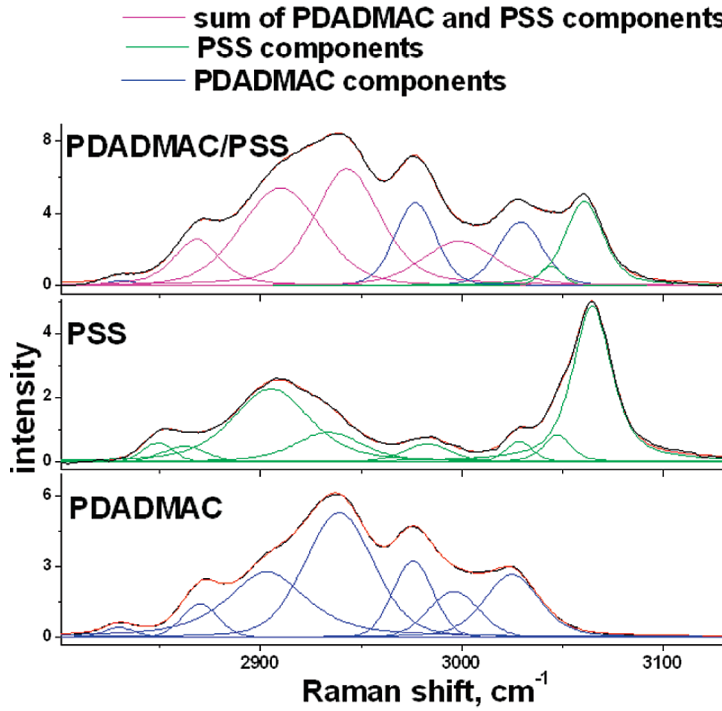

Figure 2. Raman spectral decomposition of PDADMAC/PSS complexes and their components. Black and red lines denote the recorded spectra and their fits, respectively.

Therefore, it can be concluded that the stoichiometric ratio of the complexes was n^{PAH}:n^{PSS} = 1:2 [monomer/monomer], because PAH has two CH_2 groups per monomer, while PSS has only one CH_2 group per monomer. Almost identical spectra were obtained for the mixture of PAH and PSS regardless of whether the initial mixing ratio was 1:5 or 1:3. The stoichiometry of the complexes was thus independent of the initial proportions of polycations and polyanions, provided PSS was added in sufficient excess.

The stoichiometry of the PDADMAC/PSS complexes was obtained in the same way as for PAH/PSS. Figure 2 shows the spectra decomposition of the PDADMAC/PSS complexes and the spectra of the two components: PDADMAC and PSS. The ratio of PDADMAC to PSS was n^{DADMAC}:n^{PSS} = 1:2.3 [monomer/monomer].

The stoichiometry of the complexes may depend on the conformational freedom of the polymers and on how well polycations and polyanions entangle together. Those charges, which are not compensated by the charges of the oppositely charged polyelectrolyte species, will be compensated by small counterions. The complexes formed with an excess of PSS can thus be visualized as being close to neutral in their interior, but negatively charged at their outer surface. These negatively charged sulfonic acid groups will serve as the binding sites for TTAB.

2. PSS−TTAB Complexes. Raman spectra of TTAB in solution and the dry state are presented in Figure 3. The figure provides information on the C−C skeleton vibration in the frequency regime between 1040 and 1160 cm^{-1} and the CH stretching modes of methylene and methyl groups in the range between 2700 and 3100 cm^{-1}. The spectra of TTAB in solution reflect a typical micelle structure.[29] In the micellar phase, Raman spectra are dominated by broad bands similar to what is observed in hydrocarbon liquids.[30] The broad bands centered around 2890 and 2930 cm^{-1} are two Fermi resonance bands between the asymmetric CH_2 stretching band (2882 cm^{-1} for crystalline phase) and CH_2 bending overtones (2 × 1441 cm^{-1}

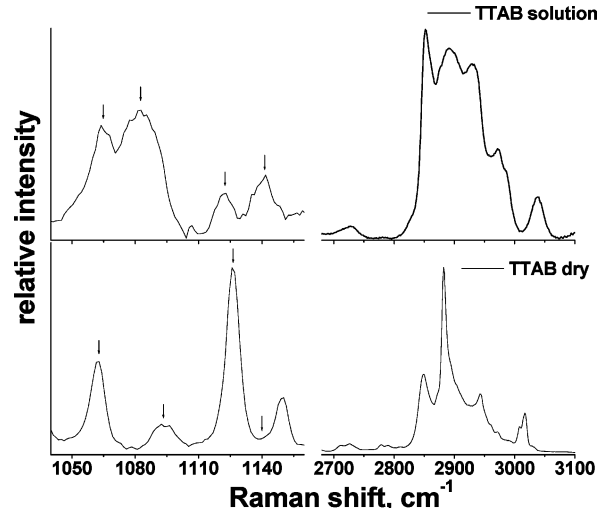

Figure 3. Raman spectra of TTAB in aqueous solution (top) and dry state (bottom).

and 2 × 1465 cm^{-1}). On the contrary, in the crystalline phase, the spectral bands of dry TTAB become sharp lines. In the C−C skeleton frequency region, the arrow marked bands (Figure 3) carry information about the conformation of the alkyl chain. The C−C stretching modes 1064 and 1123 cm^{-1} are assigned to the trans configuration of the alkyl chain, while C−C modes 1088 and 1140 cm^{-1} are responsible for gauche conformers.[30,31] The alkyl chains in the micelles exhibit a coiled liquid-like configuration with a similar amount of C−C bonds in trans and gauche conformation.[31] A strong reduction of the gauche conformers is observed in Figure 3 for the dry TTAB, indicating that the surfactant molecules arrange in a crystal lattice.

TTAB forms complexes with PSS. The Raman spectra of PSS/TTAB complexes were measured at different TTAB mole fractions in PSC. The spectra of dry TTAB/PSS complexes for TTAB percentages ranging from 0% to 67% are plotted in Figure 4. The spectra were normalized using the PSS band at

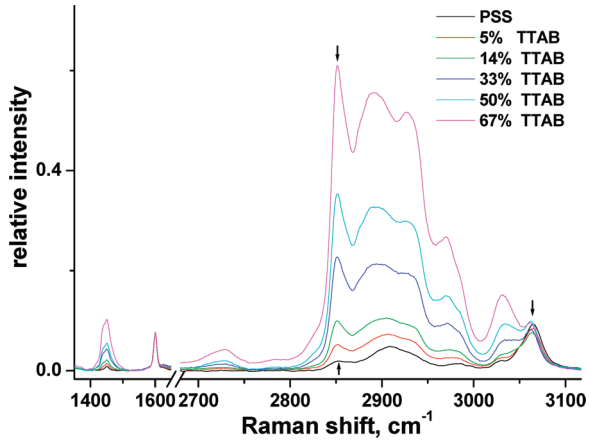

Figure 4. Raman spectra of dry PSS/TTAB complexes at different surfactant mole fractions.

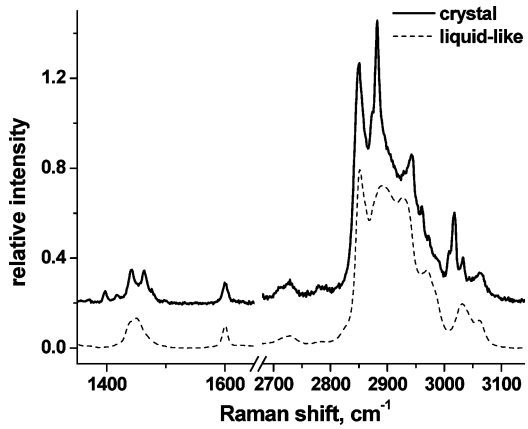

Figure 5. The phase transition of the PSS-bound TTAB from liquid-like to crystal phase at a surfactant mole fraction of 67%.

1600 cm^{-1} ($\nu(CCH)_{ringquadrant}$) as the reference band, because it does not overlap with the spectra of TTAB. The increase in the intensity of the TTAB band, $\nu_s(CH_2)$ = 2850 cm^{-1}, with increasing surfactant mole fraction can be clearly observed in Figure 4. At a TTAB mole fraction of 67% in PSC, which corresponds to 2 TTAB molecules per 1 PSS monomer, a transition from a coiled liquid-like alkyl chain configuration of the PSS associated surfactant to a crystalline phase was detected (Figure 5). The presence of a phase transition follows from the splitting into several peaks of the bands corresponding to the CH bending region (around 1450 cm^{-1}) and the appearance of sharp peaks in the stretching region. The two bands, trans band at 1064 cm^{-1} and gauche band at 1088 cm^{-1}, were chosen to estimate the decrease of gauche conformers of PSS-bound surfactant at the phase transition. These bands do not overlap with PSS bands. The ratio of the integral intensity of the chosen bands for bound TTAB corresponds to that of free TTAB in both phases.

PSS destroyed the surfactant ordering in the PSS/TTAB complexes at small surfactant concentration. While in the dry state free TTAB is in a crystalline state, a coiled liquid-like phase was observed for bound TTAB in dry PSC (Figure 4). The phase transition to the crystalline state occurred at a 2:1 mol ratio (surfactant to PSS). It can be thus concluded that the coverage of PSS by TTAB becomes saturated at this molar ratio. One can assume that a following increase of the TTAB mole fraction in the complexes leads to the growth of the crystalline phase of surfactant, which is not associated with PSS.

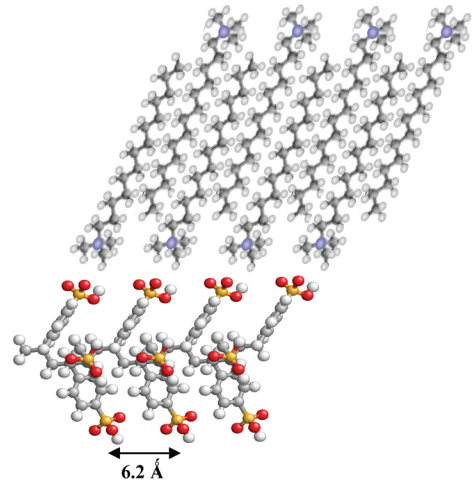

Figure 6. Side view of PSS/TTAB complexes. The red, yellow, blue, gray, and light gray balls correspond to O, S, N, C, and H atoms, respectively.

From these considerations follows that 2 TTAB molecules bind to every sulfonic acid group of the side chain of PSS. One TTAB molecule compensates with its quaternary ammonium group the negative charge of the sulfonic acid. If the second TTAB molecule would also interact with its headgroup with the sulfonic acid, the resulting complex would be rather hydrophobic. This situation would be also unfavorable from an electrostatic point of view. Therefore, we propose that the second TTAB molecule associates with its chain to the chain of the already bound first TTAB molecule in an antiparallel fashion. Such an arrangement will result in a net positive charge of the PSS/TTAB complex. This situation bears some similarity with overcharging occurring during polyelectrolyte multilayer formation.

The hypothesis of two molecules of surfactant per monomer of sulfonic acid is confirmed by molecular considerations. The distance between two sulfonic acid side chains along the axis of the molecule has been calculated to be about 6.2 Å.[32] Such a distance would be sufficient to accommodate two TTAB molecules. A scheme of the proposed arrangement of PSS and TTAB molecules is shown in Figure 6.

The spectra of the TTAB/PSS complexes have been decomposed to separate the contribution of TTAB from PSS. Three bands denoted in Figure 4 by arrows, the symmetric CH_2 stretching band of TTAB at 2850 cm^{-1}, and the corresponding band of PSS located at 2853 cm^{-1}, as well as the aromatic PSS band at 3064 cm^{-1}, were selected for calculating the TTAB content in the PSC. The contribution of the symmetric CH_2 stretching components from PSS and TTAB cannot be separated. Therefore, the sum of both was used in the following calculation of the relative contribution of TTAB (I_{rel}(TTAB)) to the spectra of the complex:

$$I_{rel}(\mathrm{TTAB}) = [I_{TTAB}(\nu_s(CH_2)) + I_{PSS}(\nu_s(CH_2))]/[I_{PSS}(\nu_{aromatic}(CH))] = A + I_{TTAB}(\nu_s(CH_2))/I_{PSS}(\nu_{aromatic}(CH))$$

where A is a constant and $I_{TTAB}(\nu_s(CH_2))$, $I_{PSS}(\nu_s(CH_2))$, and $I_{PSS}(\nu_{aromatic}(CH))$ are integral intensities of symmetric CH_2 stretching components from TTAB, PSS, and the aromatic band of PSS, respectively.

The relative TTAB intensity was plotted as a function of the TTAB mole fraction in the complexes in Figure 7. Two different branches can be observed in the plot depending on the phase

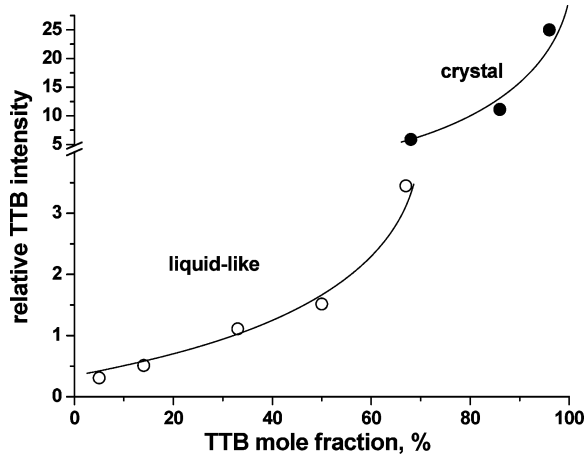

Figure 7. Relative TTAB intensity as a function of the TTAB mole fraction for the two phases: liquid-like (○) and crystal (●).

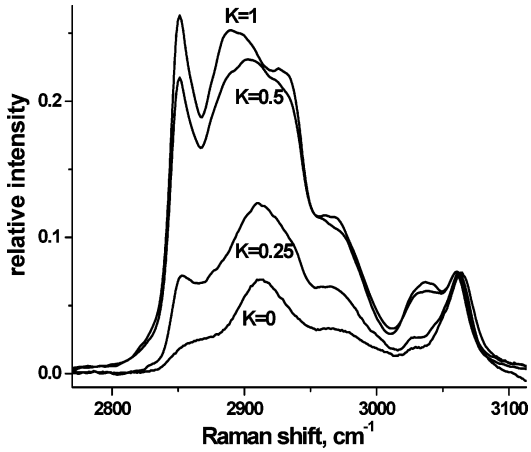

Figure 8. Raman spectra of dry PAH/PSS complexes with TTAB at different surfactant molar factors, K. Value $K = 0$ corresponds to PAH/PSS complexes without TTAB.

state of TTAB: one at high TTAB mole fractions corresponding to the crystal phase and one related to the liquid-like phase at lower TTAB contents. This curves will be used further below as calibration curves for the quantification of the amount of TTAB bound to PSS/PDADMAC and PSS/PAH complexes. This is possible because the binding of TTAB to the complexes occurs only with PSS.

3. Interaction of TTAB with PAH/PSS and PDADMAC/PSS Complexes. TTAB was added to PAH/PSS and PDADMAC/PSS complexes at different concentrations given below as molar ratios of TTAB per PSS monomers in complexes: molar ratio $(r) = n^{\mathrm{TTAB}}{:}n^{\mathrm{PSS}}$ [molecule:monomer]. Centrifugation/washing cycles were again used to remove unbound TTAB micelles from the complexes. Figure 8 presents the spectra of dry PAH/PSS complexes with TTAB at different relative molar ratios, K, of TTAB. K is defined as the relative molar ratio $K_i = r_i/r_{max} = n_i^{\mathrm{TTAB}}/n_{max}^{\mathrm{TTAB}}$, where the index "max" denotes the maximum surfactant concentration used in the experiment. K is a normalized molar ratio, which describes the increase of the surfactant mole fraction from $K = 0$, corresponding to polyelectrolyte complexes without surfactant, to $K = 1$, corresponding to the maximum surfactant concentration. The spectra of the PSC were normalized using the PSS band at 1600 cm^{-1}. Figure 8 shows that the integral intensity of the surfactant band $\nu_s(CH_2) = 2850$ cm^{-1} steeply grows with increasing TTAB molar factor up to a K value of 0.5. Further increasing the TTAB concentration up to $K = 1$ increased the intensity of the CH_2 stretching band only slightly. From this follows that the amount of bound TTAB molecules to the polyelectrolyte complexes saturates with an increasing molar ratio of TTAB to PSS in the complex.

Figure 9 shows the spectra in the CH stretching region for two different PE complexes with and without TTAB. The mole fraction of TTAB bound to the PSS in PE complexes has been determined using the spectral decomposition and the calibration curve provided in Figure 7. It is noticeable that the TTAB band intensity at $\nu_s(CH_2) = 2850$ cm^{-1} grows while the $\nu_{aromatic}(CH) = 3064$ cm^{-1} band of PSS decreases with increasing TTAB molar fractions.

The saturation of the surfactant binding for the two complexes, PAH/PSS and PDADMAC/PSS, is quantified in Figure 10. It displays the fraction of TTAB bound to the polyelectrolyte complexes as a function of the TTAB molar factor.

The most interesting finding is that the TTAB saturation on PSS in PAH/PSS and PDADMAC/PSS complexes was reached at molar fractions of 50% and 67%, respectively. A saturation value of 50% corresponds to one surfactant molecule per one PSS monomer in the PAH/PSS complex. Taking into account that the stoichiometry of the PAH/PSS complex was 1:2 and that the complex remains stable, it follows that only every second sulfonate group can serve as a potential binding site for TTAB. 50% saturation as compared to the case of free PSS thus corresponds exactly to the binding of two molecules of TTAB per every free sulfonate group. This situation is illustrated in Figure 11. The surfactants bound to PSS in PAH/PSS complexes furthermore reveal a coiled liquid-like spectrum as shown in Figure 8. A phase transition does not occur.

For the PDADMAC/PSS complex, the situation is quite different. The TTAB molar fraction reaches a plateau at 67%, which corresponds to the binding of two surfactant molecules to each PSS monomer. Because in the complex with PDADMAC roughly every second sulfonate group is utilized for binding PDADMAC, this would mean that about 4 TTAB molecules bind to a free PSS monomer in the complex. Such a conclusion contradicts the model presented in Figure 7. Therefore, the only possibility to explain the binding ratio is that the PDADMAC/PSS complexes become disassembled by TTAB and the observed 2:1 ratio corresponds to binding of TTAB to free PSS (Figure 6). Furthermore, when the surfactant threshold is reached (see arrow in Figure 10), a phase transition to the crystalline phase occurs. This corresponds to the same TTAB mole fraction of about 67% as in TTAB/PSS complexes. The spectral features of surfactant bands in the crystalline phase are identical to those of TTAB/PSS complexes (Figure 5). This similar behavior provides further evidence for the disassembling effect of TTAB, when interacting with PDADMAC/PSS complexes.

Because, on the contrary, PAH/PSS complexes remained stable, it can be concluded that the interaction of TTAB with PSS is stronger than the interaction of PSS with PDADMAC, but weaker than the interaction of PSS with PAH. This finding is consistent with the observation that TTAB is able to decompose polyelectrolyte multilayers composed of PDADMAC/PSS but not those consisting of PAH/PSS.[26]

The head groups of the TTAB are quaternary amines, being the same as the charged sites in PDADMAC. Consequently, the electrostatic part of the interaction between TTAB and the sulfonic acid groups in PSS has to be similar in strength to the interaction of latter with the quaternary amines of PDADMAC. In this case, sterical considerations may play an additional role for the dissembling. The comparatively small TTAB may possibly get

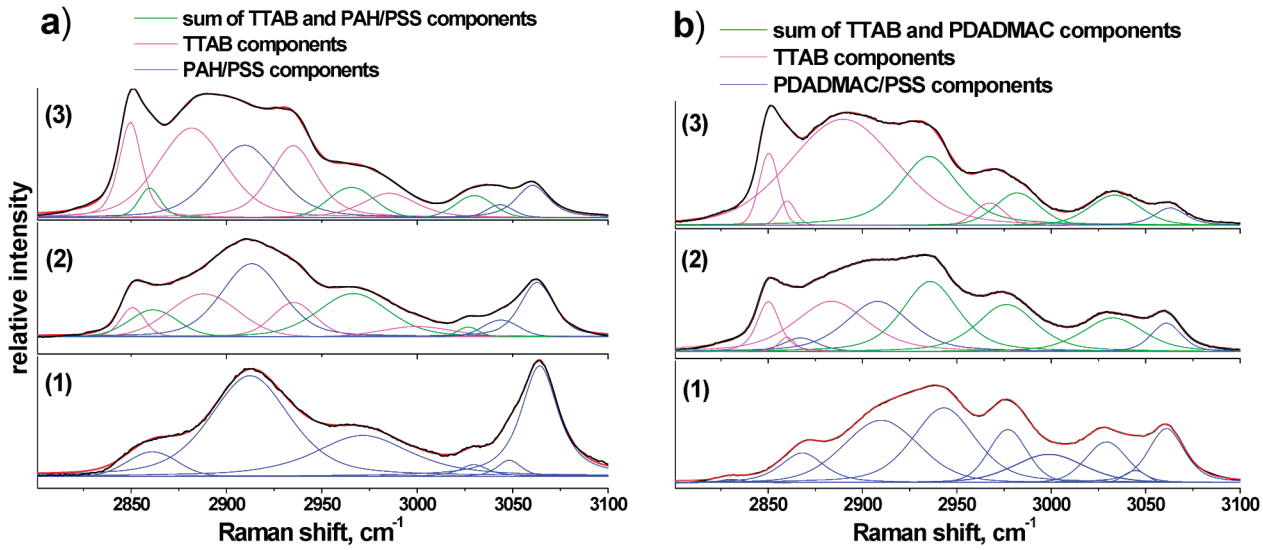

Figure 9. (a) Raman spectra of PAH/PSS without (1) and with surfactant at TTAB molar fractions of 25% (2) and 53% (3); (b) Raman spectra of PDADMAC/PSS without (1) and with surfactant at TTAB molar fractions of 33% (2) and 66% (3). The black and red lines denote the recorded spectra and their fits, respectively. The green bands are the superposition of TTAB and PE complexes spectral components, which have the same spectral location.

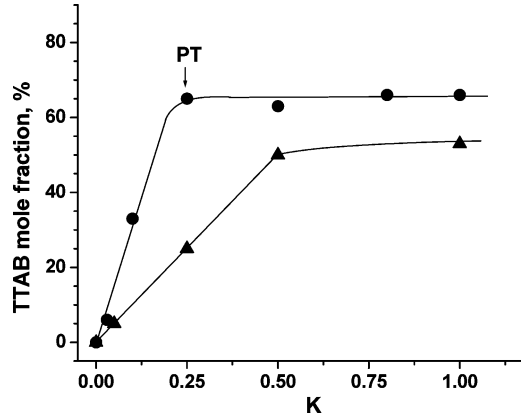

Figure 10. Saturation of surfactant binding to PSS in PAH/PSS (▲) and PDADMAC/PSS (●) complexes. The phase transition region is indicated by the arrow for PDADMAC/PSS complexes.

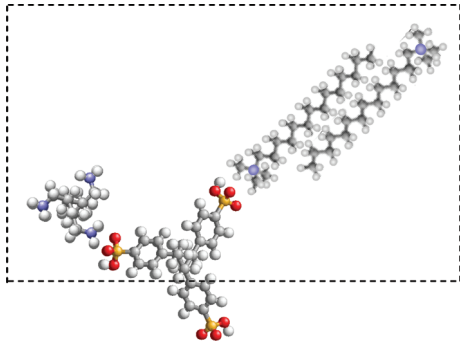

Figure 11. Front view of PAH/PSS complex (stoichiometry 1:2) interacting with TTAB. The molar ratio of surfactant to PSS is 1:1 (TTAB mole fraction is 50%). The red, yellow, blue, gray, and light gray balls correspond to O, S, N, C, and H atoms, respectively.

direct access to each monomer of the PSS, while the PDADMAC PSS interaction may suffer from conformational constraints. PAH/PSS complexes remained stable upon addition of TTAB, which confirms data obtained by measurements with polyelectrolyte multilayers.[26] The PAH charges are provided by primary amines, which interact with the sulfonic acid groups. This interaction is obviously stronger than that with the

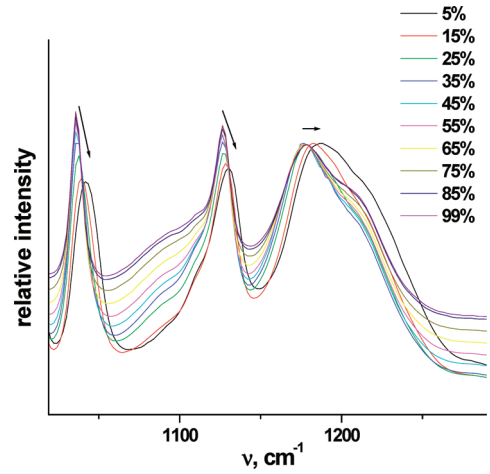

Figure 12. ATR-FTIR humidity scans of PSS from 99% to 5%.

quaternary amines of TTAB. This is consistent with the behavior of PE multilayers, where it has been evidenced that the PAH/PSS multilayers have a stronger interlayer interaction than PDADMAC/PSS multilayers.[33−35] The question, however, remains: why the interaction of primary amines with the sulfonic acid is stronger than that of the quaternary amines with the sulfonic acid? To better understand the nature of these interactions, we studied the influence of water on the TTAB polyelectrolyte interaction in a more systematic way.

4. Role of Water. Figure 12 shows ATR-FTIR spectra of PSS recorded at different humidities. The vibrations of the sulfonate group, which is sensible to humidity, were analyzed. The vibrational spectra of sulfonate groups have been studied in detail, and their assignment can be found in various papers.[36−38] Decreasing the water content induced a blue shift of the vibrational bands $\nu_{as}(SO_3^-)$ from 1177 to 1187 cm^{-1}, $\nu_s(SO_3^-)$ from 1039 to 1045 cm^{-1}, and $\nu(SO_2)$ from 1128 to 1133 cm^{-1}. The arrows denote the blue shift in Figure 12. This is the typical dehydration behavior of groups that are forming hydrogen bonds with water. The same blue shift upon dehydration was seen when the Raman spectrum of the dry state was compared to the spectrum in solution.

In Figure 13 have been plotted the maxima of the Raman $\nu(SO_2)$ and the $\nu_s(SO_3^-)$ vibrations bands in the dry state as a

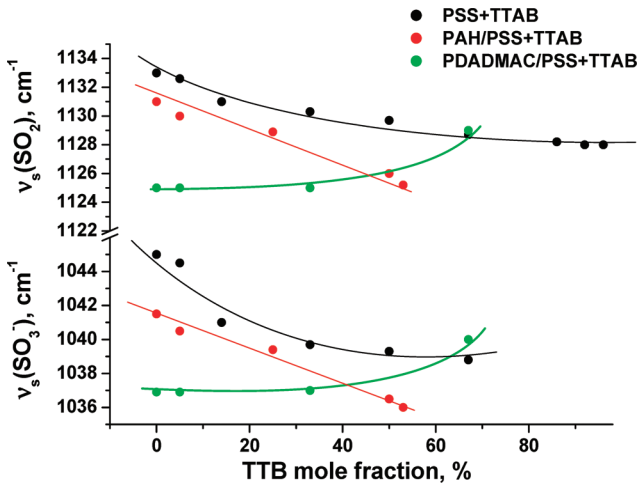

Figure 13. Maxima of the vibrational frequencies corresponding to the sulfonate groups as a function of TTAB mole fraction for PE complexes with surfactant recorded by Raman in dehydrated state.

function of the mole fraction of TTAB for mixtures of TTAB with PSS, PSS/PAH, and PSS/PDADMAC complexes. The major findings were that the addition of TTAB reverses the dehydration-induced blue shift characteristic for PSS. In the case of PAH/PSS complexes, it even becomes overcompensated.

The reverse effect was observed for PDADMAC/PSS complexes. For low to medium fractions of TTAB, the frequency remained almost constant. Yet at saturation molar fractions of about 67%, the frequency increased to values corresponding to the case of free PSS, which we again associate with the disassembly of the complex by TTAB.

In Figure 14 are compared the values of the $\nu(SO_2)$ and $\nu_s(SO_3^-)$ for PSS, PSS/PDADMAC, PSS/PAH, alone, or with TTAB (saturation region) for the dry and the fully hydrated state. A frequency decrease with growing surfactant concentration was observed for PSS and PAH/PSS complexes (Figure 14). As it can be observed in Figure 14, dry PSS/TTAB complexes display the same frequency as if the complex would be in the hydrated state, $\nu_s(SO_3^-) = 1039$ cm^{-1} and $\nu(SO_2) = 1128$ cm^{-1}. Therefore, it can be concluded that the quaternary ammonium ion carrying three methyl groups excluded water from the sulfonate group, rendering its frequency independent of the state of hydration.

Figure 14 allows for a comparison of the degree of dehydration of the different complexes. For the PAH/PSS complex, the dehydration effect was remarkably smaller than for PSS alone. We therefore suppose that the binding of PAH and PSS removes some water from the sulfonate group by forming hydrogen bonds between the primary amines and the oxygens of the sulfonate. This extra interaction on top of the electrostatic interaction may contribute to the exceptional stability of the PAH/PSS interaction sites. This would be a remarkable point, because the PAH/PSS multilayer system is one of the most studied multilayers and has been considered as the characteristic example for electrostatic interaction as the basis for multilayer assembly.

Another interesting finding is that in the presence of TTAB in PAH/PSS complexes, the observed vibrational frequencies of the sulfonate groups in the dehydrated state are lower than in the hydrated state. This behavior is opposite to the one observed for the complex without TTAB. We suppose that the interaction of TTAB with PSS removes water from sulfonate groups. This may cause a change in the conformation of the PAH/PSS complex, because the sulfonic acid groups become more hydrophobic, when the sulfonic acid charge is compensated by TTAB. It is possible that as a result of these conformation changes certain topological restrictions are overcome, and some sulfonate groups may get closer to the primary amino groups of the PAH. This situation could result in the formation of additional hydrogen bonds between the amino groups of PAH and sulfonic acid groups, which have not been close enough to each other before surfactant addition. This would explain the comparatively small frequency in the dry state. The addition of TTAB thus would induce a stronger interaction between PAH and PSS.

As can see from Figure 14 for PADMAC/PSS complexes, the dehydration had no effect on the vibration frequencies of the sulfonate groups. The quaternary ammonium ion carries three methyl groups generating a hydrophobic environment for the sulfonic acid groups. It is thus quite conceivable that the quaternary amine replaced water molecules from the sulfonate group and prevents the formation of hydrogen bonds. Therefore, the vibrational properties of the sulfonate group in the PSS/PDADMAC complex become independent of the state of hydration. This behavior is very similar to the interaction of PSS with TTAB as discussed further above.

Conclusions

The spectroscopic study of polyelectrolyte complexes interacting with TTAB provided new insights in the interac-

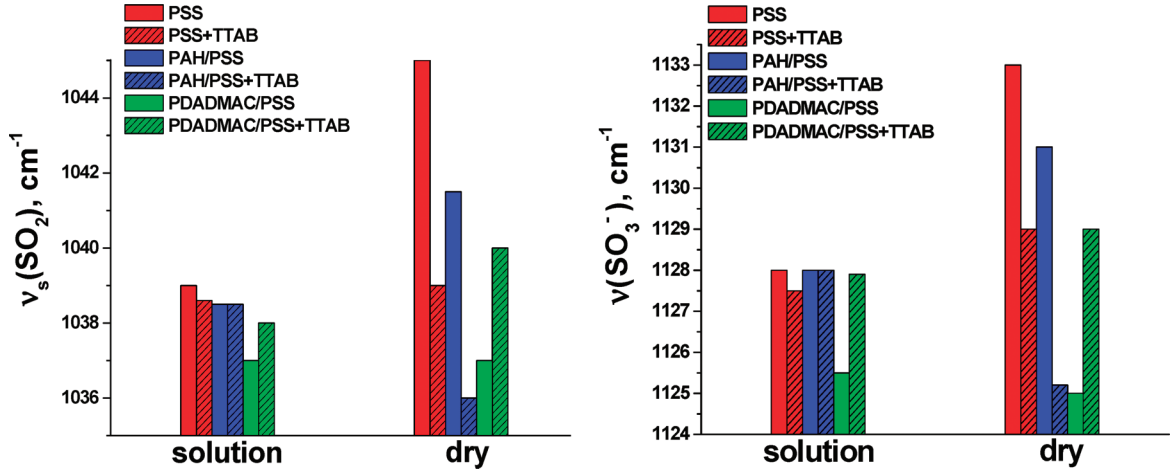

Figure 14. The sulfonate frequencies bar diagram in hydrated and dehydrated states for PSS and its complexes with polycations in the presence and absence of TTAB. The surfactant mole fraction was 67% where saturation occurs.

tion between PAH and PSS as well as between PDADMAC and PSS and the interaction of polyanions with quaternary ammonium surfactants. The stoichiometry of PSS/PAH complexes and PSS/PDADMAC complexes was independent of the amount of PSS and polycation provided there is sufficient excess of PSS in the mixture. In the dry state, TTAB bound to PSS assumes a coiled liquid-like alkyl configuration up to saturation at a molar fraction of 67%. At higher concentrations, the TTAB shows a transition to a crystalline phase. A molar fraction of 67% TTAB/PSS is equivalent to binding of 2 molecules of TTAB per sulfonic acid group. One of the TTAB molecules compensates the charge of the sulfonic group, while the other assembles in an antiparallel orientation providing to the complex charge and stability in the aqueous environment. Another important conclusion is that TTAB interacting with PSS in PDADMAC complexes is capable of disassembling the latter. This is in agreement with the effect of TTAB on multilayers.[26]

Spectroscopic measurements performed at different humidities showed that the dry PSS/PAH complexes display the $\nu(SO_2)$ and $\nu_s(SO_3^-)$ bands at positions that are indicative of the presence of hydrogen bonds between PSS and PAH. Further red shifts of these bands when mixing the PSS/PAH complexes with TTAB point to structural rearrangements of the complex, resulting in an increased amount of hydrogen bonds between amino and sulfonate groups. The formation of hydrogen bonds would explain the stability of the complexes of PSS/PAH in the presence of TTAB. The importance of hydrogen bonds for the PAH/PSS assembly has been underestimated in the past. It may account for the exceptional stability of multilayers of PAH/PSS. It may further be an important factor influencing the permeability, the mechanics, and other properties of PAH/PSS multilayers and capsules.

References and Notes

(1) Langevin, D. *Adv. Colloid Interface Sci.* **2001**, *467*, 89–90.
(2) Langevin, D. *Adv. Colloid Interface Sci.* **2009**, *170*, 147–148.
(3) Antonietti, M.; Thünemann, A. *Curr. Opin. Colloid Interface Sci.* **1996**, *1*, 667.
(4) Sabaté, R.; Estelrich, J. *Int. J. Biol. Macromol.* **2001**, *28*, 151.
(5) Grueso, E.; Roldan, E.; Sanchez, F. *J. Phys. Chem. B* **2009**, *113*, 8319.
(6) Mitra, D.; Bhattacharya, S. C.; Moulik, S. P. *J. Phys. Chem. B* **2008**, *112*, 6609.
(7) Winnik, F.; Regismond, S. T. A.; Picullel, L.; Lindman, B.; Karlstrom, G.; Zana, R. *Polymer Surfactant Systems*; Dekker: New York, 1998; Vol. 77, pp 65−142, 267−316, 409−454.
(8) Mantzaridis, C.; Mountrichas, G.; Pispas, S. *J. Phys. Chem. B* **2009**, *113*, 7064.
(9) Norrman, J.; Lynch, I.; Piculell, L. *J. Phys. Chem. B* **2007**, *111*, 8402.
(10) Picullel, L.; Lindman, B. *Adv. Colloid Interface Sci.* **1992**, *41*, 149.
(11) Taylor, D. J. F.; Thomas, R. K.; Penfold, J. *Adv. Colloid Interface Sci.* **2007**, *132*, 69–110.
(12) Staples, E.; Tucker, I.; Penfold, J.; Warren, N.; Thomas, R. K.; Taylor, D. J. F. *Langmuir* **2002**, *18*, 5147.
(13) Campbell, R. A.; Ash, P. A.; Bain, C. D. *Langmuir* **2007**, *23*, 3242.
(14) Nizri, G.; Magdassi, S. *J. Colloid Interface Sci.* **2005**, *291*, 169.
(15) Vaknin, D.; Dahlke, S.; Travesset, A.; Nizri, G.; Magdassi, S. *Phys. Rev. Lett.* **2004**, *93*, 218302.
(16) Nizri, G.; Lagerge, S.; Kamyshny, A.; Major, D. T.; Magdassi, S. *J. Colloid Interface Sci.* **2008**, *320*, 74.
(17) Sasaki, S. *J. Phys. Chem. B* **2007**, *111*, 8453.
(18) Sokolov, E. L.; Yeh, F.; Khokhlov, A.; Chu, B. *Langmuir* **1996**, *12*, 6229.
(19) Nizri, G.; Makarsky, A.; Magdassi, S.; Talmon, Y. *Langmuir* **2009**, *25*, 1980.
(20) Zhang, M. N.; Su, L.; Mao, L. Q. *Carbon* **2006**, *44*, 276.
(21) Liu, Y.; Jiang, W.; Li, S.; Li, F. *Appl. Surf. Sci.* **2009**, *255*, 7999.
(22) Döbbelin, M.; Arias, G.; Loinaz, L.; Llarena, I.; Mecerreyes, D.; Moya, S. E. *Macromol. Rapid Commun.* **2008**, *29*, 871.
(23) Dvoracek, C. M.; Sukhonosova, G.; Benedik, M. J.; Grunlan, J. C. *Langmuir* **2009**, *25*, 10322.
(24) Liu, X.; Zhou, L.; Geng, W.; Sun, J. *Langmuir* **2008**, *24*, 12986.
(25) Samokhina, L.; Schrinner, M.; Ballauff, M. *Langmuir* **2007**, *23*, 3615.
(26) Iturri, J. J.; Llarena, I.; Moya, S. E.; Donath, E. *Macromol. Rapid Commun.*, **2009**, *30*, 1756−1761.
(27) Estrela-Lopis, I.; Leporatti, S.; Clemens, D.; Donath, E. *Soft Matter* **2009**, *5*, 214.
(28) Gorski, N.; Kalus, J. *Langmuir* **2001**, *17*, 4211.
(29) Kalyanasundaram, K.; Thomas, J. K. *J. Phys. Chem.* **1976**, *80*, 1462.
(30) Snyder, R. G. *J. Chem. Phys.* **1967**, *47*, 1316.
(31) Haramagatti, C. R.; Islamov, A.; Gibhardt, H.; Gorski, N.; Kuklin, A.; Eckold, G. *Phys. Chem. Chem. Phys.* **2006**, *8*, 994.
(32) Donath, E.; Walther, D.; Shilov, V. N.; Knippel, E.; Budde, A.; Lowack, K.; Helm, C. A.; Möhwald, H. *Langmuir* **1997**, *13*, 5294.
(33) Picart, C.; Senger, B.; Sengupta, K.; Dubreuil, F.; Fery, A. *Colloids Surf., A* **2007**, *303*, 30.
(34) Gao, C.; Donath, E.; Moya, S.; Dudnik, V.; Möhwald, H. *Eur. Phys. J. E* **2001**, *5*, 21.
(35) Gao, C.; Leporatti, S.; Moya, S.; Donath, E.; Möhwald, H. *Langmuir* **2001**, *17*, 3491.
(36) Whittington, D.; Milar, I. R. *J. Appl. Chem.* **1968**, *18*, 122.
(37) Grumelli, D.; Bonazzola, C.; Calvo, E. J. *Electrochem. Commun.* **2006**, *8*, 1353.
(38) Edwards, H. G. M.; Brown, D. R.; Dale, J. R.; Plant, S. *J. Mol. Struct.* **2001**, *595*, 111.

JP908608U